La mer 34: 192–198, 1996
Société franco-japonaise d'océanographie, Tokyo

Tidal energy in Suyoung Bay, Korea

Dong-Sun KIM* and Tetsuo YANAGI*

Abstract: To investigate the characteristic of M_2 tide, tidal current and tidal energy in Suyoung Bay of Korea, we developed two-dimensional numerical model under the cartesian co-ordinate. The maximum speed of M_2 tidal current is about 30cm s^{-1} at the north-eastern and south-western part of the bay. M_2 tidal energy flux in Suyoung directs from the north-east to the sout-west. The maximum values of M_2 tidal energy flux are seen at the south-eastern and north-eastern part of the bay and M_2 tidal energy loss by bottom friction at unit area in Suyoung Bay is 34 ergs s^{-1} cm^{-2}.

1. Introduction

Suyoung Bay is situated at the south-eastern coastal area of Korea where the topography gradually widens and deepens from the mouth of Suyoung River to off-shore. It is a coastal plain type estuary whose shape is nearly triangle. The inner bay water mass is directly subjected to the intrusion of the off-shore water mass (Fig. 1).

By the report of the Pusan City of Korea (1984), the semi-diurnal tidal component is distinguished and the tidal form number (K_1+O_1/M_2+S_2) is 0.11~0.17 in Suyoung Bay. The average tidal range is about 101cm, 36cm in spring and neap tide, respectively. The amplitude of M_2 tide is 34.3cm and that of S_2 tide is 16.4cm.

Until now, the studies about tide and tidal current have been carried out by KIM and HAN (1982), JUNG and YOA (1992), KIM and LEE (1991, 1992) and HWANG (1993) but there has been no study on the tidal energy in Suyoung Bay. Therefore, in this study, we try to make clear the characteristic of M_2 tide, tidal current and to inquire about the M_2 tidal energy in Suyoung Bay.

2. Numerical model of tide & tidal current

The equations used in this numerical simulation are the horizontal two-dimensional momentum and continuity equations for tide and tidal current in the homogeneous fluid under the cartesian co-ordinate which are as follows (YANAGI and OKAMOTO, 1985),

$$\frac{\partial \bar{u}}{\partial t}+(\bar{u}\cdot\nabla)\bar{u}+fK\times\bar{u} = -g\nabla\eta-\frac{\gamma_b^2|\bar{u}|\bar{u}}{H+\eta}+\nu\nabla^2\bar{u} \quad (1)$$

$$\frac{\partial \eta}{\partial t}+\nabla\cdot\{(H+\eta)\bar{u}\} = 0 \quad (2)$$

where $\bar{u}$ is the depth-averaged velocity vector, t the time, ∇ the horizontal differential operator, f ($=2\Omega\sin\Phi$: $\Omega=7.27\times10^{-5}$sec^{-1} and $\Phi=35°07'$ N) the Coriolis parameter, K the locally vertical unit vector, g ($=980$ cm sec^{-2}) the gravitational acceleration, η the surface elevation above the mean sea level, γ_b^2 ($=2.6\times10^{-3}$) the bottom frictional coefficient, H the local depth, v ($=5.0\times10^5$cm^{2}s^{-1}) the horizontal eddy viscosity.

Equations (1) and (2) are approximated by finite-differences and are solved by the primitive method (YANAGI *et al.*, 1983). Depths used for this model were taken from Korean hydrographic chart No. 201C. The maximum depth is 54 m and the calculation grid size is 0.2 km×0.2 km. For the computational stability of numerical calculation, the time interval according to Courant-Friedrichs-Lewy criterion (MESINGER and ARAKAWA, 1976) is 5 sec in this study.

* Department of Civil and Ocean Engineering, Ehime University, Matsuyama 790, Japan

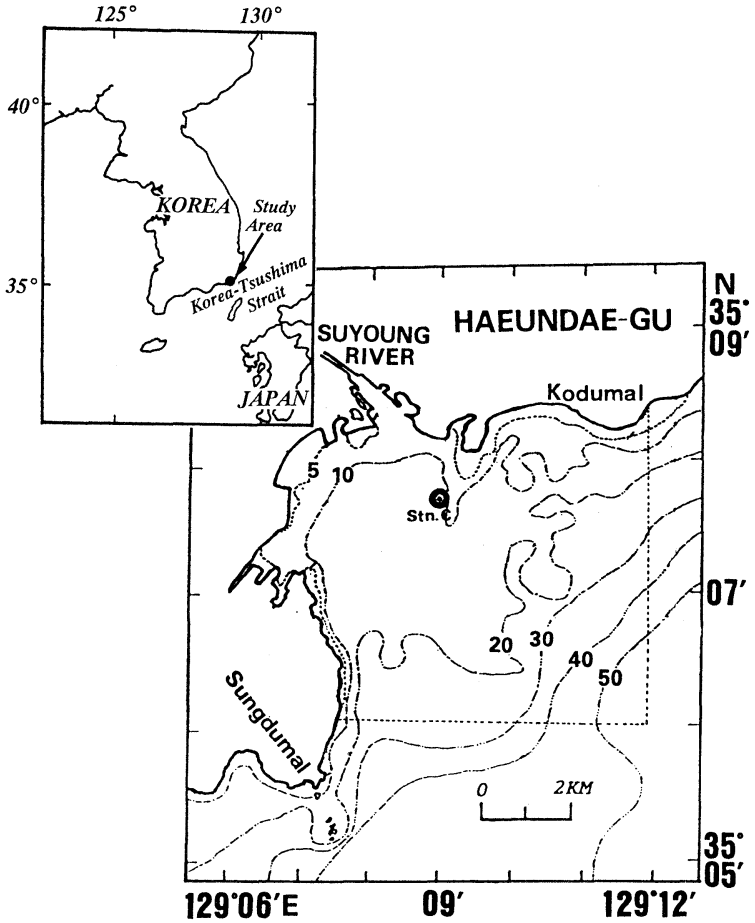

Fig. 1. Map of the study area where Stn. C is the current observation station. Broken line shows the open-boundary of numerical model. Numbers show the depth in meter.

Along the eastern open-boundary (129° 12'E), the M_2 tidal amplitude decreases from 34cm to 32cm toward the north and the phase decreases from 235° to 233° in the same direction. The phase at the southern open-boundary (35° 06′ N) is 236°. As for the amplitude along the southern open-boundary, it decreases from 35cm to 34cm toward the east (ODAMAKI, 1989). M_2 tidal wave propagates from the north-eastern part to the south-western part of Suyoung Bay.

The quasi-steady state is obtained four tidal cycles after the beginning of the calculation and the harmonic analysis of sea surface elevation and current field is carried out at the 5th tidal cycle.

3. Results

The calculated results of amplitude and phase of M_2 tide and tidal current are shown in Fig. 2. The amplitude and phase of M_2 tide is about 34cm and 234° at the mouth of river, respectively. The amplitude of M_2 tital current is about 40cm s^{-1}at the outer bay and about 1 cm s^{-1} at the mouth of river. The phase of M_2 tidal current is 330° at the southern part of the bay and about 270° at the mouth of river. From this figure, we can understand that M_2 tidal wave behaves like a standing wave at the central part of Suyoung Bay because the phase difference between tide and tidal current is near 90°. The comparision of calculated M_2 tidal current ellipse and observed one (KIM *et al.*, 1991)

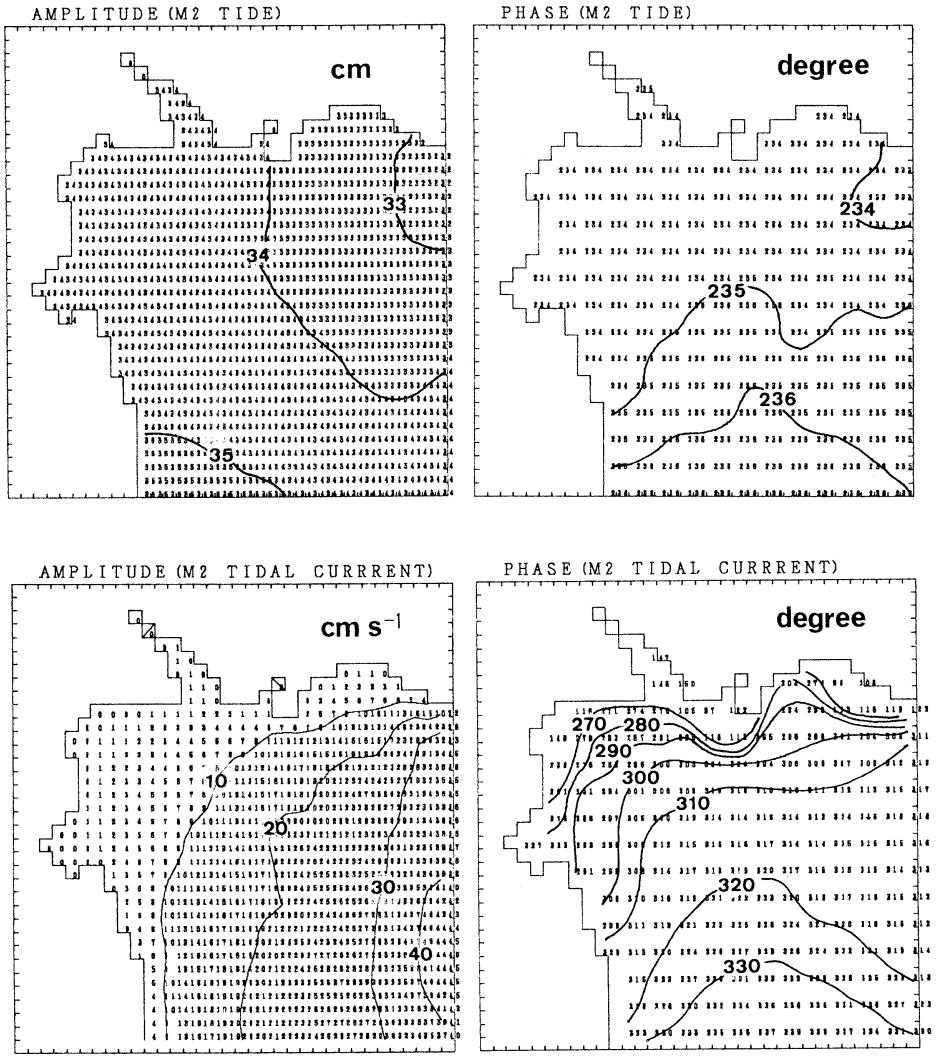

Fig. 2. Calculated amplitude (left) and phase (right) of M_2 tide (upper) and M_2 tidal current (lower). Phase is reffered to the transit of Moon at 135° E.

at Stn. C (see Fig. 1) is shown in Fig. 3. The dotted circle shows the observed result 3 m below the surface of Stn. C, and the full circle the calculated one. The calculated M_2 tidal current ellipse by our model well reproduces the observed one in speed and direction.

The flow patterns of M_2 tidal current at the times of maximum flood and ebb at the central part of the bay are shown in Fig. 4. The M_2 tidal current at the maximum flood flows from the north-east toward the south-west. The tidal current at the inner bay flows parallel to the coastal line and the speed at the inner bay is slower than that at the outer bay. Generally, the flow pattern of M_2 tidal current at the maximum ebb is opposite to that of maximum flood.

The calculated tide-induced residual current by M_2 tidal current, which is obtained by averaging calculated tidal current over one-tidal cycle, is shown in Fig. 5. Tide-induced residual current by M_2 tidal current makes two circulations in the bay, that is, one is the eastward flow at the north-eastern part and the other is the southward flow at the southwestern part.

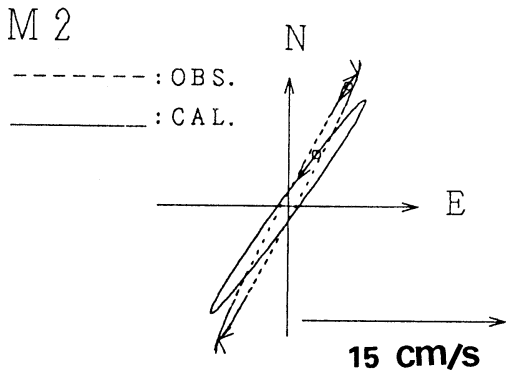

Fig. 3. Observed (full line) and calculated (dotted line) of tidal current ellipses at Stn. C.

4. Tidal Energy

The tidal energy flux through the n-th grid is estimated as follows (YANAGI *et al.*, 1982),

$$E_n^{\circ}\frac{g}{2}V_nH_n\cos\Phi_n^{VH} \qquad (3)$$

where V_n is the amplitude of tidal volume transport through the n-th grid, H_n the tidal amplitude at the n-th grid, and Φ_n^{VH} the phase difference between the tidal volume transport and the tidal elevation.

The vector average of tidal energy flux through each grid gives an indication of the direction and magnitude of tidal energy flow associated with M_2 tidal component. These vectors are shown in Fig. 6 (a). There is a noticeable reduction in tidal energy flux near the shallower area. It is shown that M_2 tidal energy in Suyoung Bay is from the north-eastern part toward the south-western part and this is the same as the tidal wave propagation. Fig. 6 (b) shows the tidal energy flux which is intergrated at the eastern and southern boundaries. The tidal energy flux through the eastern boundary and that through the southern boundary are 4.69×10^{13}ergs s^{-1}, 3.11×10^{13} ergs s^{-1}, respectively. Therefore the tidal energy of 1.58×10^{13} ergs s^{-1} is lost in Suyoung Bay.

On the other hand, the M_2 tidal energy dissipation can be directly estimated by the following formula (TAYLOR, 1919),

$$E^{f^*}=\frac{4}{3\pi}\times\gamma_b^2\times S\times\left(\frac{V}{A}\right)^3 \qquad (4)$$

Here γ_b^2 is the bottom frictional coefficient ($=2.6\times10^{-3}$), S the surface area of each grid, A the cross sectional area of each grid, V the amplitude of tidal volume transport across each grid. The application of this formula to the Irish sea (TAYLOR, 1919) demonstrated that the tidal energy flow from the ocean tides into a partially enclosed body of water was principally dissipated by the bottom friction. The distribution of M_2 tidal energy dissipation due to bottom friction in Suyoung Bay is shown in Fig. 7. The maximum values of M_2 tidal energy dissipation are seen around the south-eastern and the

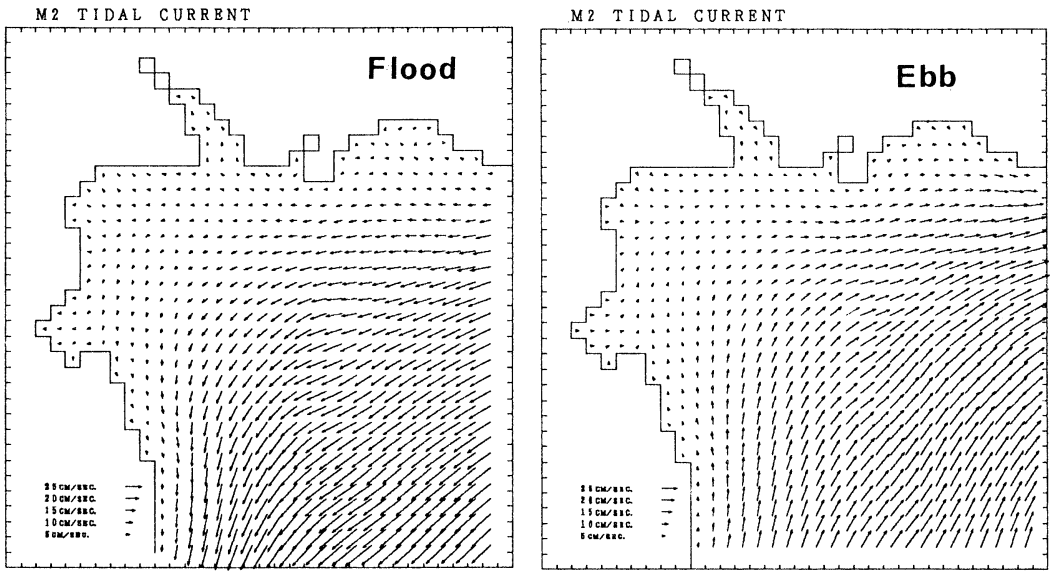

Fig. 4. Maximum flood (left) and ebb (right) M_2 tidal current.

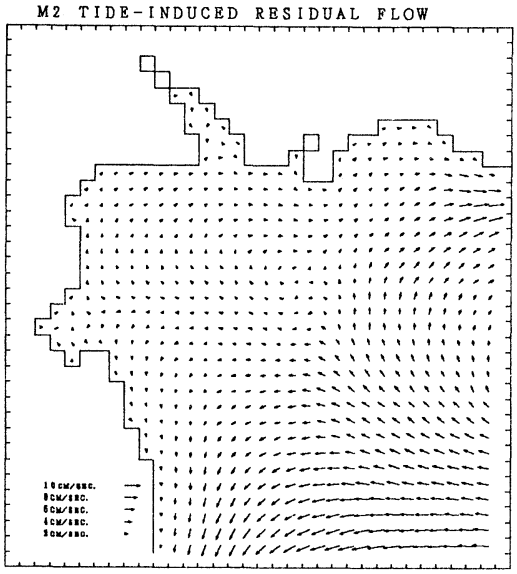

Fig. 5. Calculated tide-induced residual current by M_2 tidal current.

north-eastern part of the bay. The total M_2 tidal energy dissipation due to bottom friction is 1.03×10^{13} ergs s^{-1} in Suyoung Bay. The difference of M_2 tidal energy flux between the eastern and the southern boundaries (1.58×10^{13} ergs s^{-1}) is nearly the same as the calculated result ($=1.03\times10^{13}$ ergs s^{-1}) by Eq. (4). This fact shows the propriety of the M_2 tidal energy calculation of Eq. (3).

5. Discussion

We developed two-dimensional numerical model under the cartesian co-ordinate in Suyoung Bay of Korea, compared its results with that of field observation and calculated the M_2 tidal energy. The calculated M_2 tidal current by our model well reproduces the observed one in speed and direction. The tide-induced residual current, generated by the M_2 tidal current, is eastward and southward flow around the north-eastern and south-western part, respectively.

The comparision of M_2 tidal energy in Suyoung Bay, Korea and the Seto Inland Sea, Japan (YANAGI *et al.*, 1982) is shown in Table 1. The maximum values of M_2 tidal energy flux in Suyoung Bay are seen around the south-eastern and north-eastern part. The M_2 tidal energy flux in Suyoung Bay directs from the north-east to the south-west. On the other hand, local maximum values of M_2 tidal energy flux in the Seto Inland Sea are seen around the Sea of Iyo and Akashi Strait (YANAGI *et al.*, 1982). The topography of Suyoung Bay is monotonous that is gradually widens and deepens from the mouth of Suyoung River to off-shore (see Fig. 1). On the other hand, the topography of the Seto Inland Sea is very complicated (see Fig. 8) and that causes very strong tidal current, especially near the straits. The maximum

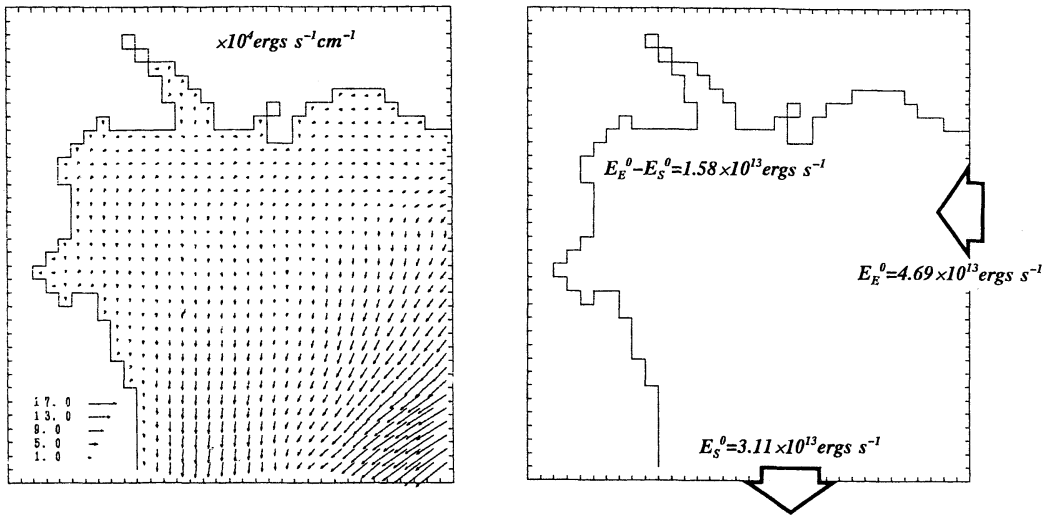

Fig. 6. M_2 tidal energy flux vectors (a) and the M_2 tidal energy flux at the eastern and the southern boundaries (b).

Table 1. M_2 tidal energy loss per unit area (E), M_2 tidal energy flux (E°), M_2tidal energy dissipation due to friction (E^{f*}), amplitude of tidal volume transport (V), and cross sectional area (A) in the Suyoung Bay and Seto Inland Sea.

	E ergs s^{-1} cm^{-2}	E° ergs s^{-1}	E^{f*} ergs s^{-1}	V cm^3 s^{-1}	A km^2
Suyoung Bay	34	4.69×10^{13} (East Bound.) 3.11×10^{13} (South Bound.)	1.03×10^{13}	3.26×10^{9} (East Bound.) 3.17×10^{9} (South Bound.)	0.17 (East Bound.) 0.16 (South Bound.)
Seto Inland Sea	189	37.4×10^{15} (Bungo Ch.) 9.5×10^{15} (Kii Ch.)	41.6×10^{15}	15×10^{12} (Bungo Ch.) 2×10^{12} (kii Ch.)	12.5 (Bungo Ch.) 3.1 (Kii Ch.)

*Surface Area : Suyoung Bay ($30km^2$), Seto Inland Sea ($22{,}000km^2$)

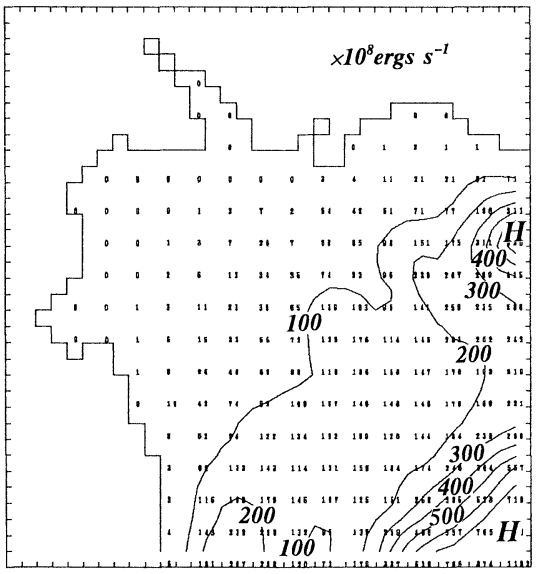

Fig. 7. Distribution of M_2 tidal energy dissipation due to bottom friction.

amplitude of M_2 tidal current in Suyoung Bay is about 40cm s^{-1} and that in the Seto Inland Sea is about 500 cm s^{-1} at Naruto Strait. The cross sectional area in Suyoung Bay is about 87 times smaller than that of the Seto Inland Sea. Hence the amplitude of tidal volume transport in Suyoung Bay is about 3 order of magnitude smaller than that of the Seto Inland Sea. The M_2 tidal energy loss per unit area is about 34 ergs $s^{-1}cm^{-2}$ in Suyoung Bay and 189 ergs s^{-1} cm^{-2} in the Seto Inland Sea; the value of Suyoung Bay is about 5.5 times smaller than that of the Seto Inland Sea. The dissipation rate of tidal energy by bottom friction, which represents the rate of work per unit area made by the flowing water column against bottom friction, is large at the limited area like straits. That is to say, the tidal energy loss per unit area near the starits, where a strong tidal current exists, is larger than elsewhere. In the Seto Inland Sea, the tidal energy loss per unit area is about 400 ergs s^{-1} cm^{-2} at the vicinity of Tsurushima Strait, about 411 ergs $s^{-1}cm^{-2}$ at the southern area of Naruto Strait and about 532 ergs $s^{-1}cm^{-2}$ at the western part of Akashi Strait, especially a local maximum value about 17,021 ergs s^{-1} cm^{-2} around the Kurushima Strait (YANAGI *et al.*, 1982). These values are about 2~90 times larger than the average M_2 tidal energy dissipation per unit area in the Seto Inland Sea.

Therefore, we consider that the difference of M_2 tidal energy loss per unit area due to bottom friction in Suyoung Bay and the Seto Inland Sea is produced by the interaction of tidal current with horizontal and bottom topography.

Acknowledgments

The authors express their sincere thanks Dr. H. TAKEOKA and Mr. H. AKIYAMA of Ehime University for their useful discussions. The calculation was carried out on a FACOM M770 of the Computer Center of Ehime University.

References

HWANG, J. D. (1992): Dispersion of pollutant flowing into Suyoung Bay. Department of Oceanography, Graduate School, National Fisheries University of Pusan, 44p (in Korean).

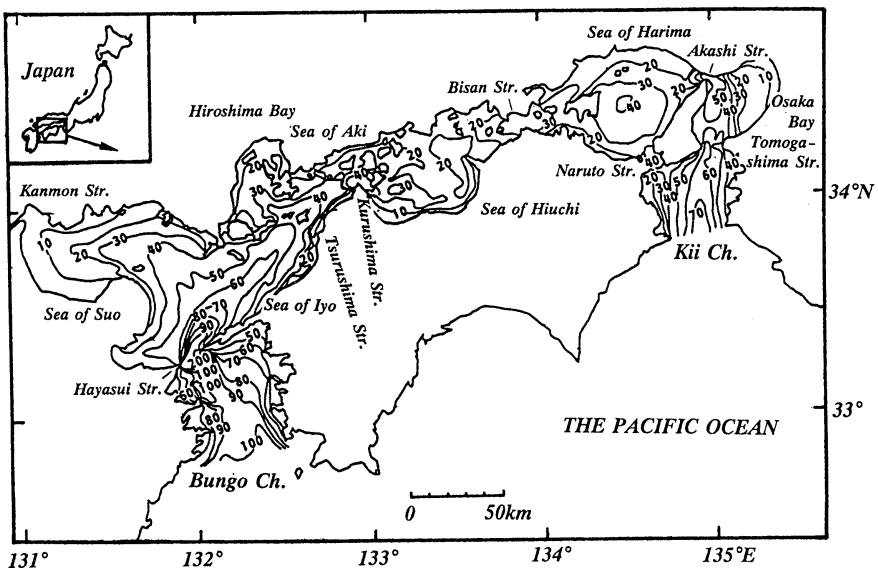

Fig. 8. Bathymetric map of the Seto Inland Sea, Japan. Numbers show the depth in meter.

JUNG, Y. C. and S. J. YOA (1992): Numerical Modelling on Hydrodynamics and Diffusion in Suyeong Bay. Bull. Korean Fish. Soc. **25** (2), 133–143 (in Korean).

KIM, C. J. and J. S. LEE (1991): A study on the flowing and diffusion of sea water by two-level numerical model in the estuary. Bull. Korean Fish. Soc. (1), **24**, 59–69 (in Korean).

KIM, C. J. and J. S. LEE (1992): Distributions of Tidal Curent, Salinity and Suspended Sediment in Suyoung Bay. Bull. Korean Fish. Soc. **25** (5), 359–370 (in Korean).

KIM, D. S. and K. D. CHO and B. G. LEE (1991): Seasonal variation of oceanic conditions in Suyoung Bay. Bull. Korean Fish. Tech. Soc. **27**, 105–119 (in Korean).

KIM, Y. S. and Y. H. HAN (1982): A study in the Characteristics of the Circulation and Diffusion in Suyeong Bay. Bull. Korean Fish. Tech, Soc. **18** (2): 55–61 (in Korean).

MESINGER, F. and A. ARAKAWA (1976): Numerical Methods used in atmospheric Models. GARP (Global Atmospheric Research Programe) Publication Series No.14, WMO-ICSU Joint Organizing Committee, 64p.

ODAMAKI, M (1989): Tides and Tidal Current in the Tsusima Strait. J. Oceanogr., **45**, 65–82.

Pusan City of Korea (1984): A report of numerical and mathematical model experiments of the development area in Suyoung Bay. 398p (in Korean).

TAYLOR, G. I. (1919): Tidal friction in the Irish Sea, Phil, Trans. Roy. Soc., **A220**, 1–193.

YANAGI, T. and H. TAKEOKA and H. TSUKAMOTO (1982): Tidal Energy Balance in the Seto Inland Sea. J. Oceanogr. **38**, 293–299.

YANAGI, T. TSUKAMOTO, H. INOUE and T. OKAICHI (1983): Numerical simulation of drift card dispersion. La mer, **21**, 218–224.

YANAGI, T and Y. OKAMOTO (1985): A numerical simulation of oil spreading on the sea surface. La mer, **22**, 137–146.

Received January 5, 1996
Accepted March 29, 1996